INTERNATIONAL JOURNAL ON INFORMATICS VISUALIZATION

journal homepage : www.joiv.org/index.php/joiv

Classification of Sugarcane Area Using Landsat 8 and Random Forest based on Phenology Knowledge

Sudianto Sudianto [a,*], Yeni Herdiyeni [b], Lilik Budi Prasetyo [b]

[a] *Department of Informatics, Institut Teknologi Telkom Purwokerto, 53147, Indonesia*
[b] *Department of Computer Science, IPB University, Bogor, 16680, Indonesia*
[c] *Department of Forest Resources Conservation & Ecotourism, IPB University, Bogor, 16680, Indonesia*
Corresponding author: [*]sudianto@ittelkom-pwt.ac.id

***Abstract*—Indonesia is one of the largest countries globally with an area for planting sugarcane. The current problem is that determining the planting area of sugarcane is still done conventionally; this is very limited and wastes time. Thus, knowing the sugarcane planting area becomes essential for policymaking through Remote Sensing technology. However, the challenge of Remote Sensing is the limited data due to weather and the spectral variability of other plants. So, it is necessary to classify based on phenological knowledge. The study aims to classify sugarcane areas based on phenological knowledge using Remote Sensing and Machine Learning. This application finished on the cloud platform Google Earth Engine (GEE) through Landsat 8 satellite imagery data. The knowledge of sugarcane phenology was built based on the Normalized Difference Vegetation Index (NDVI) spectral value and built with the harmonic model. In addition, classification is accomplished by object-oriented (OO) methods for segmentation classification. Object-oriented is solved by the Simple Non-Iterative Clustering (SNIC) algorithm for spatial cluster identification, the Gray-Level Co-occurrence Matrix (GLCM) for texture extraction, and the Random Forest algorithm for Land Use-Land Cover (LULC) classification. The results of the accuracy analysis using the confusion matrix and the classification of sugar cane areas based on phenological knowledge obtained the best results with an overall accuracy of 95.9% with a Kappa coefficient of 0.92. It can be concluded that a classification approach with knowledge of plant phenology can help better classify the availability of land for plantations in the future.**

***Keywords*— Classification; GEE; Landsat 8; Object-Oriented; Phenology; SNIC GLCM.**

Manuscript received 17 Nov. 2022; revised 25 Apr. 2023; accepted 4 Jun. 2023. Date of publication 30 Nov. 2023.

I. Introduction

Indonesia is a country that has the seventh-largest sugarcane planting area in the world [1]. Sugarcane as a raw material for sugar is a strategic commodity for the economy in Indonesia, with an area of around 440 thousand ha in the 2014-2018 period [2]. Indonesian sugarcane production is dominated in East Java at around 58.92%, with 14.54% in Kediri Regency [1]. As a basic need and a relatively popular source of calories, sugar production made from Indonesian sugarcane is supplied around 51.15% of the area of East Java Province [2]. So this makes East Java Province the center of sugarcane cultivation in Indonesia.

As support for modern agriculture, ensuring the availability of sugarcane cultivation in a wide area can be done automatically, precisely using remote sensing combined with artificial intelligence to classify sugarcane areas. In particular, remote sensing with satellites provides effective methods due to its unique spectral, temporal, and spatial resolution [3]. From previous research, remote sensing users with satellite technology have been applied to support sugarcane farming, e.g., SPOT-5 High-Resolution Geometrical (HRG), Landsat-7 Enhanced Thematic Mapper Plus (ETM+), Advanced Spaceborne Thermal Emission and Reflection Radiometer (ASTER), ENVISAT Advanced SAR (ASAR), High-Resolution Imaging Camera (CCD), and Moderate Resolution Imaging Spectroradiometer (MODIS). To estimate sugarcane yield, map the area of sugarcane crops' area and differentiate sugarcane varieties [3]–[8]. However, previous classification studies still ignore phenology factors affecting the classification results. Much less the challenge of using remote sensing technology is limited data due to cloudy weather. In addition, the characteristics of the heterogeneous landscape (various spectral variations of other plant species) complicate the extraction of sugarcane information [9]. Phenology sugarcane is unique and different from other plants, e.g., rice or tobacco. Sugarcane has a phenology of 10-12 months.

Thus, information on sugarcane phenology is beneficial as a reference for remote-sensing image data. Because remote sensing with suitable time-series data can produce different land cover (sugarcane planting area) from other types of variability [10]. Thus, as an alternative to the classification of sugarcane areas based on phenological knowledge.

The paradigm shift of expensive and sophisticated computing has now been replaced by cloud computing and free. In this respect, Google's platform, Google Earth Engine (GEE), is powerful for solving various challenges in cloud-based geospatial analysis very efficiently and processing data, processing, storage, and integration [11]. On the GEE cloud platform, users can access and analyze spatial data anytime, anywhere via a user-friendly web with an effective scripting language and cloud-free data sets without limitations on storage space or computational resource images [12]–[14]. In this case, remote sensing applications can be implemented in GEE, for example, creating Land Use-Land Cover (LULC) physical of the earth's surface (i.e., rocks, grasslands, water) or maps of agriculture or residential areas [15]. The abased approach object is applied to Land Use-Land Cover (LULC) for sugarcane area classification [16]. Object-oriented objects have a geographic appearance, such as shape and length, so it is necessary to extract the texture [17]. So, GEE provides a Simple Non-Iterative Clustering (SNIC) algorithm that helps identify the potential of each object and group similar pixels [18]. Object-oriented generally classify objects by combining spatial, spectral, and texture information in the image. GEE also provides the Gray-Level Co-occurrence Matrix (GLCM) for obtaining texture information. The GLCM texture is also helpful in enhancing the LULC classification by combining vegetation indices and multispectral bands [19]. Then, non-parametric Machine Learning, such as Random Forest (RF), was applied to the LULC classification because of its efficient and accurate results on remote sensing images [20], [21].

In solving existing problems. This study classified sugarcane areas by considering plant phenological knowledge in determining datasets. Determining datasets is crucial for the accuracy of an area mapping, especially for the limitations of datasets that are categorized as feasible due to natural factors. So, it is hoped that through plant phenology knowledge, the ability to map sugarcane areas with limited datasets can be resolved and mapping accuracy to be more precise.

Therefore, this research aims to classify sugarcane areas based on phenological knowledge. The object-oriented classification technique approach is carried out by applying the SNIC and GLCM algorithms and using the Machine Learning (Random Forest) algorithm to classify the final object on the GEE code. GEE can perform classification settings for various parameters (e.g., selecting input lines, selecting classification algorithms, RF tests, and various segmentation scales). Meanwhile, accuracy tests (overall accuracy and kappa coefficient) were conducted through the confusion and visual matrices.

In participating in the discussion in this paper, the author compiles systematically: materials and methods, which explain the location of the research and ways to obtain knowledge about the phenology of sugarcane plants. In addition, preprocessing to ensure that the image data used is correct. Then, the results section explaining phenological knowledge is used as a basis for mapping sugarcane plant areas with the Random Forest algorithm. Finally, a conclusion explaining the accuracy of the classification of sugarcane areas, as well as suggestions for subsequent research.

II. Materials and Method

A. Study Area

The study area is in PT Perkebunan Nusantara X (PTPN X), as shown in Fig 1, between the sub-district Ploso Klaten and Ngancar, Djengkol Kediri, part of East Java Province, Indonesia. Djengkol Kediri has a tropical climate with an annual temperature between 23°C to 31°C with an average rainfall rate of about 1,652 mm per day. In addition, the field of this area is relatively flat, with a mean altitude of about 284 m aloft sea level, and is located in (Lat: 112.1469, Long: -7.9308), (Lat: 112.2065, Long: -7.9308) (Lat: 112.2065, Long: -7.8642), (Lat: 112.1469, Long: -7.8642), (Lat: 112.1469, Long: -7.9308). Djengkol Kediri is East Java province's second-largest sugarcane planting area [1]. Besides sugarcane, the primary vegetation in this area is tobacco and grass. However, the dominant plant types in the area are sugarcane [22]. This site was selected because it represents the sugarcane community in Indonesia, which needs to be monitored for sustainability to support the economy.

B. Phenology of Sugarcane

Sugarcane phenology is essential as a knowledge base [23]–[25]. Sugarcane phenology is divided into four phases: germination, tillering, grand growth, and maturity, which lasts for one phenological cycle of 10-12 months. Phenological knowledge is used as a reference in determining image data to classify sugarcane areas. Sugarcane phenological knowledge is built based on cropping pattern trends. The phenology of sugarcane in the study area from October to early November was the seeding and seedling stage, early January to late April, the period of stem elongation, the accumulation of sugar in May, June to August, the maturation stage, the harvest stage in September until the following year.

The phenological knowledge in this study was obtained from the maximum red wave absorption ability (NDVI spectral index) of sugarcane to differentiate between other crops; this is to determine the trend and seasonality of sugarcane in the study area on a per-pixel basis (Fig 2). The seasonal forecast is then built by combining the linear model with the harmonic model (Formula (1)) [26]. NDVI values (Formula (2)) were integrated and used as the basis for seasonal trend analysis (Fig 2) from image collection data for 2018–2020. The NDVI spectral index is beneficial for identifying sugarcane seasonality and providing information on sugarcane cropping patterns. The analysis of seasonal trends shows that sugarcane planting peaks from January to June, with the beginning of planting in October and ending in September of the following year (Table I). Thus, the selection of image data used for classification in this study can be seen in Table III.

$$p_t = \beta_0 + \beta_1 t + A\cos(2\pi\omega t - \varphi) + e_t = \beta_0 + \beta_1 t + \beta_2 \cos(2\pi\omega t) + \beta_3 \sin(2\pi\omega t) + e_t \quad (1)$$

$$NDVI = \frac{(NIR - Red)}{(NIR + Red)} \quad (2)$$

Image data selection is in the range of two months after seeding and two months before harvest because it can be easier to interpret in the phenological range phase. In addition, if only some image data meets the requirements (cloud-free) that include the phenology of sugarcane, then use the image data six months after seeding because the leaf area index value reaches the maximum, considering that it must guarantee the accuracy of the classification.

Fig. 1 The study area in Djengkol Kediri, Indonesia, and an overview of the sugarcane plantation (region of interest)

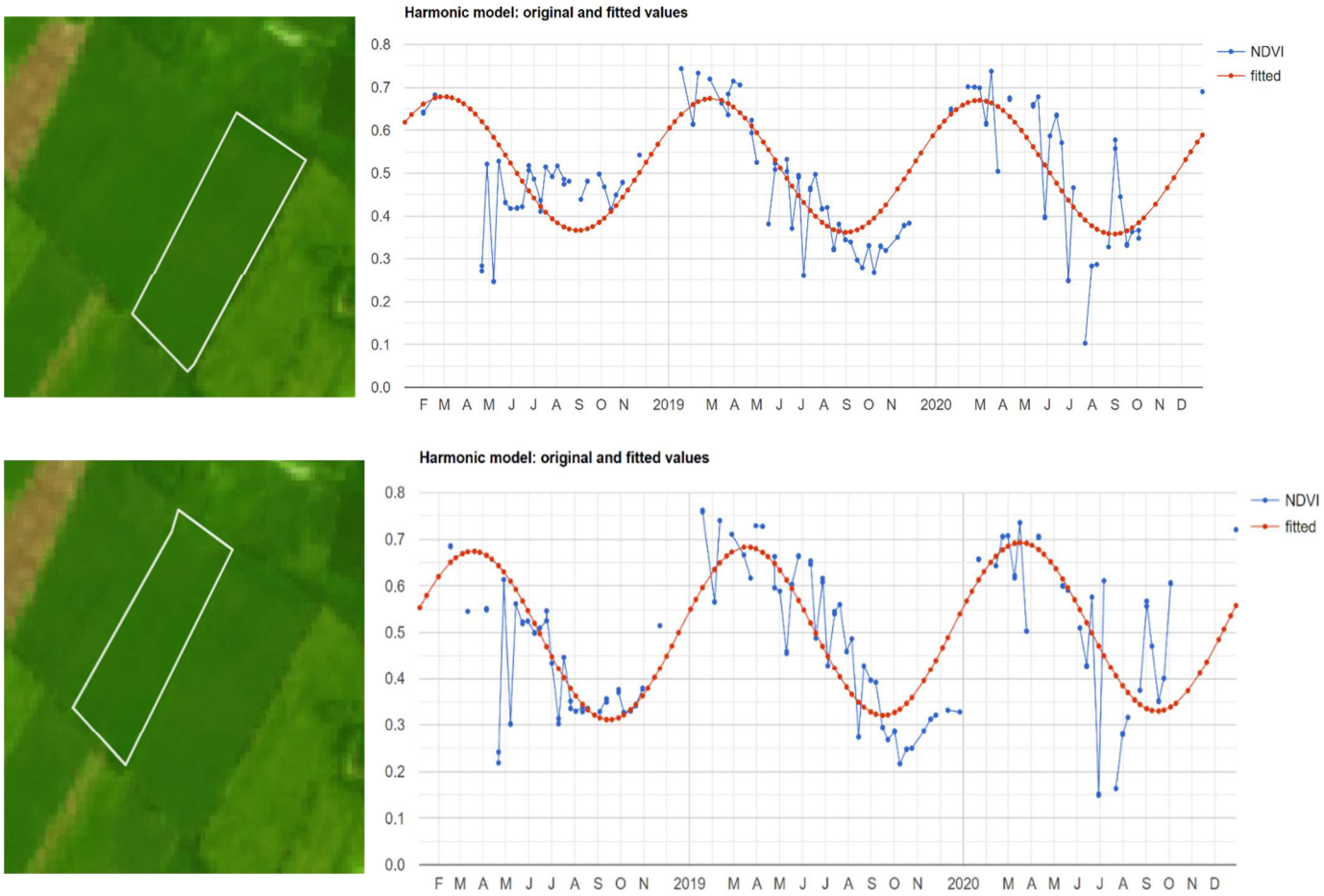

Fig. 2 The trend of sugarcane phenology in region of in field based on a region (part of the area of interest) using the harmonic model.

TABLE I
THE PERIODS OF SUGARCANE PHENOLOGICAL IN THE STUDY AREA

Crop	2019			2020								
	Oct	Nov	Dec	Jan	Feb	Mar	Apr	May	Jun	Jul	Agt	Sep
Sugarcane	SE	SE/SL	SL	ST	ST	ST	ST	SA	MA	MA	MA	HA

Note: HA: harvest stage; SE: seeding stage; SL: seedling stage; ST: stem elongation stage; SA: sugar accumulation stage; MA: maturation stage.

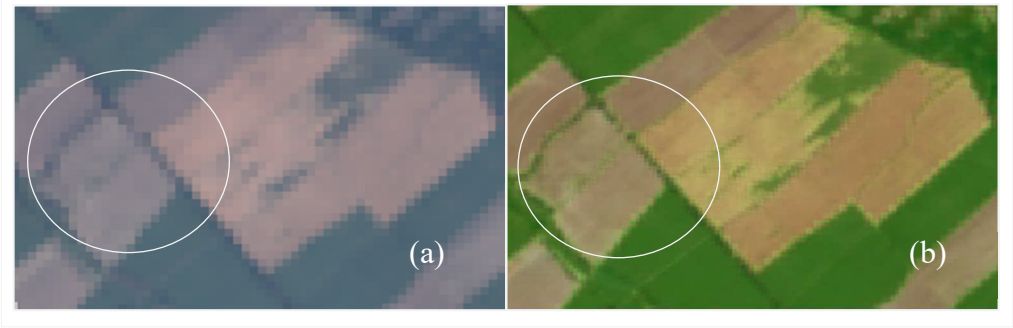

Fig. 3 The sharpens L8 resolution (a) RGB image; (b) Pan-sharpened image

C. Pre-Processing and Sample Data

This application's dataset comes from images filtered by code and specific in 2019. The initial Landsat 8 dataset was created from "LANDSAT/LC08/C01/T1_TOA", a cloud-free polygon of the region of interest (ROI). In addition, a pan-sharpening technique was also applied to sharpen the resolution by combining the panchromatic mode (Band 8) through the Brovey algorithm (which was initially 30m to 15m) [27] (Formula (3)) (Fig (3)). In addition, an index was applied: Normalized Difference Vegetation Index (NDVI) to mapping land cover change to produce an increase in classification accuracy [28], [29].

$$Red_{out} = \frac{R_{in}}{(R_{in} + G_{in} + B_{in}) \times P_{in}} \quad (2)$$

The diverse landscape mosaics of the study sites are presented with four classification classes: (1) sugarcane, composed of fragmented areas; (2) other crops, composed of small and fragmented areas such as tobacco; (3) built-up areas such as settlements and other manufactured surfaces; (4) bare soil, a planted area that is not planted. Then, to test the reliability and usability of the entire procedure, a total of 85 class sample points were identified through the GEE interface and labeled manually through visual interpretation of the same base layer as shown (Fig 4) (Table II). The labeling was done in Landsat 8 RGB through high-resolution Google Maps and infrared composite layers [30], [31]. Furthermore, the sample points were divided randomly, with 70% training and 30% validation.

Fig. 4 Overview of sample points of class label

TABLE II
THE NUMBER OF POINTS FOR EACH CLASSIFICATION CLASS

Classes	Number of Points
Built-up	7
Bare soil	24
Sugarcane	30
Other crops	24

TABLE III
COMPARISON OF DATASETS USED OF CLASSIFICATION

Based on Phenology Knowledge	Without Phenology Knowledge
Feb "LANDSAT/LC08/C01/T1_TOA/LC08_119065_20190210"	Feb "LANDSAT/LC08/C01/T1_TOA/LC08_119065_20190210"
May "LANDSAT/LC08/C01/T1_TOA/LC08_119065_20190517"	May "LANDSAT/LC08/C01/T1_TOA/LC08_119065_20190517"
Jun "LANDSAT/LC08/C01/T1_TOA/LC08_118066_20190611"	Jun "LANDSAT/LC08/C01/T1_TOA/LC08_118066_2019061"
Jul "LANDSAT/LC08/C01/T1_TOA/LC08_118065_20190713"	Jul "LANDSAT/LC08/C01/T1_TOA/LC08_118065_20190713"
	Aug "LANDSAT/LC08/C01/T1_TOA/LC08_119065_20190805"
	Sep "LANDSAT/LC08/C01/T1_TOA/LC08_118066_20191001"
	Oct "LANDSAT/LC08/C01/T1_TOA/LC08_118066_20191118"

D. Methodology

The research workflow consists of three significant steps: dataset composition, object-oriented classification, and accuracy assessment, developed in two GEE scripts (Fig 5). First, the composition of the dataset is implemented in a detached script to speed up the classification and accuracy assessment procedure because, in the next stage, the basic composite image requires adjustments. Second, the GEE script for classification and accuracy assessment is developed with an object-oriented engineering approach and applies the Random Forest classifier [32]. Then, the latter performs a confusion matrix with validation data.

1) Dataset Composition: GEE provides a collection of Landsat 8 data. The available datasets are filtered or cloud-

free. In addition, a pan-sharpening technique was also applied to sharpen the resolution by combining the panchromatic mode (Band 8). Following the process, to obtain augmentation data, the central statistics used NDVI (mean, max, and standard deviation) to produce an additional six bands loading the primary statistics of the spectrum indices used to represent the variability of the LULC class. Then, compute the median pixel value of the final composite data set for the selected band and add the index statistics of the selected spectrum among those available to the composite. Finally, export the desired ribbon from the data set. The input requirements are shown in Table IV.

TABLE IV
REQUIREMENTS TO SET FOR CREATING DATASET COMPOSITE

Requirements	Description
Region of interest (ROI)	The study site of PTPN X, Djengkol Kediri, Indonesia
Periods of Interest	Start date and end date (YYYY-MM-DD), period 2019
Bands	L8 bands selected (Band 2, Blue) (Band 3, Green) (Band 4, Red) (Band 5, NIR) (Band 6, SWIR 1) (Band 8, Panchromatic) and Create NDVI

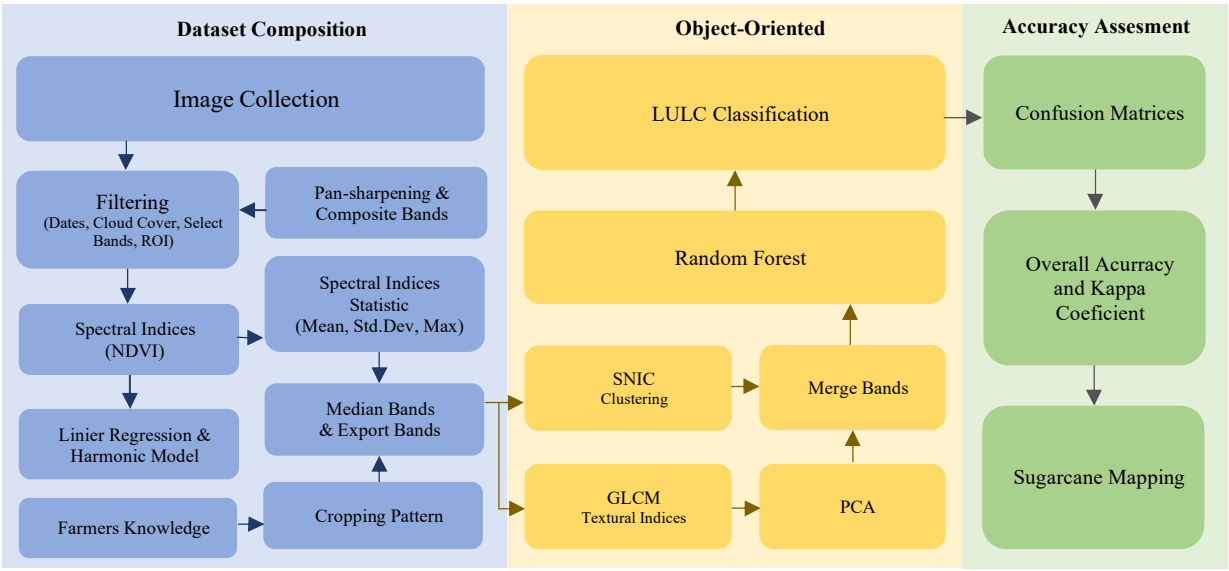

Fig. 5 Flow diagram in building sugarcane area classification with Random Forest algorithm through plant phenology knowledge

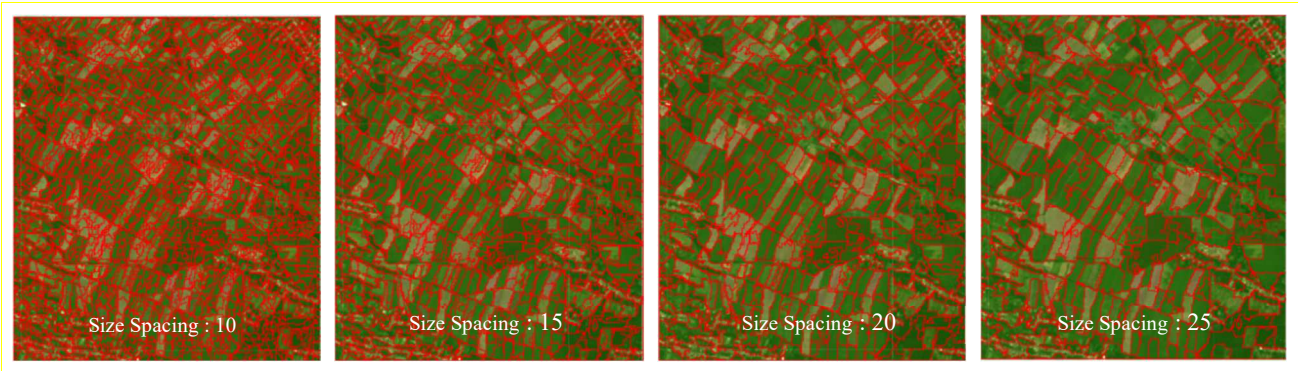

Fig. 6 Multiple size spacing of segmentation to produce maximum accuracy

2) Land Use-Land Cover Classification: In this study, performing LULC classification using a Random Forest (RF) based on supervised learning takes several inputs that can execute the code and requires information about the training points used to train the classifier [33] shown in Table V. The sample point is included in the "Newfcr" feature set for training the selected classifier. Meanwhile, the Random Forest classifier has set the number of trees to three categories: 50, 100, and 150. The object-oriented classification process is carried out by combining spatial grouping steps. It aims to group similar and contiguous pixels, compute texture index on a clustering principle, and object-based classification. This study proposes two methods combining the SNIC and GLCM algorithms implemented detached in GEE. SNIC uses a seed grid as input by "Image.Segmentation.seedGrid" function by requiring the distance of the super pixel seed location (in pixels), which affects the cluster character and can be changeable to find the best grade. Codes at the test stage using varying spacing (5, 10, 15, 20, 25, 30) are shown in Fig 6. Next, these values are identified, considering the texture of the landscape patches in the study site. To identify objects (clusters), the SNIC is subject to parameters and produces a multi-band taster (input spacing), belonging to additional layers and clusters that contain the average value of the input features. In GEE, SNIC requires the setting of several key parameters: “compactness factor” affects cluster condition (more significant values

result in extra tight clusters); "Connectivity" (4 or 8) determines the proximity of Rooks or Queen's to join adjacent groups; "NeighborhoodSize" avoids boundary artifacts. In this case, the regional characteristics are a consideration for setting parameters because the SNIC output varies depending on the visualization scale; these parameters are defined as next: neighborhood size = 256, connectivity = 8, and compactness = 0, as well as setting a 15m radius cluster output scale.

The GLCM algorithm approach uses a merger of NIR, GREEN, and RED bands on the elementary composite data to produce an image formula (4) [34] because GLCM requires an 8-bit gray-level image as input. In order to obtain a single representative band (PC first) containing most of the texture information, appropriate standardization was applied, selecting the most relevant PCA from the 7 GLCM metrics (Angular Second Moment (ASM); Contrast; Correlation; Entropy; Variance; Inverse Difference Moment (IDM); Sum Average (SAVG).) [34], [35]. After that, the mean of PC1 in a detached band is calculated for every object that belongs to the SNIC. The average band of PC1 objects is attached to the interested band from the process of segmentation SNIC. In the final part, the LULC classification is reproduced through the object-oriented approach by defining and practicing the procedure for the Random Forest classifier sourced from the dataset. Then, to speed up execution, all these stages of code are developed on the raster domain without applying conversion to the vector domain.

$$Gray = (0.3 \times NIR) + (0.59 \times Red) + (0.11 \times Green) \quad (4)$$

TABLE V
REQUIREMENTS TO SET FOR LULC CLASSIFYING

Requirements	Description
Region of interest (ROI)	The study site of PTPN X, Djengkol Kediri, Indonesia
Newfcr	A collection set labeled LULC class is then randomly divided for 70% training and 30% validation
Bands	The result of the "Dataset composition" step

III. RESULTS AND DISCUSSION

The various tests carried out in the study area and the overall accuracy results are presented in Table VI. The classification is divided into two schemes to find out the best accuracy of the proposed method: (1) composite dataset based on phenological knowledge (2) composite dataset without phenological knowledge. Classification based on phenological knowledge obtained the best overall accuracy results of 95.9% at size spacing 10, RF (100) and size spacing 10, RF (150). In comparison, the classification without knowledge of phenology obtained the best overall accuracy of 91.5% at size spacing 15, RF (50). So, from the two schemes applied, classification based on phenological knowledge is better than without phenological knowledge.

The best accuracy on datasets with phenological knowledge, tuning the number of trees 100 and 150, has the same pattern. This shows that increasing the number tree does not affect the accuracy results, and obtained the accuracy results are almost the same. Whereas in datasets without phenological knowledge, changes in the number tree value have no effect, with the overall accuracy obtained approaching the same accuracy value.

The classification results also separate sugarcane and other areas (Fig 7). From the best accuracy results, the most dominant sugarcane area ranged from 42.03% (20.350.781,318 m^2, RF 100) and 42.65% (20.653.067,433 m^2, RF 150). In addition, other class distribution areas are bare soil 17.69% and 17.87%, Other crops 35.57% and 35.34%, Built-up 4.71% and 4.14% (Fig 8).

Therefore, the classification of Land Use-Land Cover used phenological knowledge improves accuracy compared to those without sugarcane phenology knowledge. Phenology provides essential information on plants to determine the right time to use composite data as input for classifying sugarcane areas. In contrast to research [36], [37] still has not considered phenological knowledge.

Fig. 7 The map of the distribution of sugarcane area in region of interest

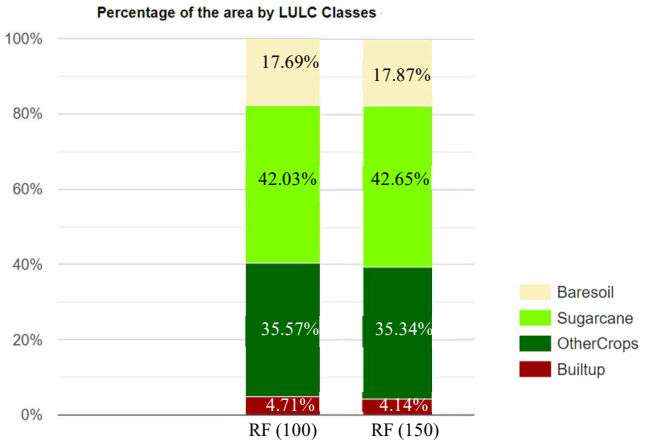

Fig. 8 The large area by classes (the best classification with phenological knowledge)

TABLE VI
OVERALL ACCURACIES AND KAPPA RESULTED FROM THE OBJECT-ORIENTED (OO) APPROACHES, FROM SATELLITE DATA LANDSAT 8, APPLYING THE RANDOM FOREST (RF) CLASSIFIER, USING DIFFERENT SIZE SPACING (5, 10, 15, 20, 25, 30)

Classifier	With Phenology Knowledge											
	Overall Accuracy (%)						Kappa Coefficient					
	5	10	15	20	25	30	5	10	15	20	25	30
RF (50)	87.3	92.3	92.0	90.1	87.9	80.5	0.81	0.89	0.88	0.86	0.80	0.72
RF (100)	88.8	95.9	90.0	86.6	87.9	76.9	0.83	0.92	0.85	0.80	0.80	0.65
RF (150)	88.8	95.9	90.0	86.6	87.9	76.9	0.83	0.92	0.85	0.80	0.80	0.65

Classifier	Without Phenology Knowledge											
	Overall Accuracy (%)						Kappa Coefficient					
	5	10	15	20	25	30	5	10	15	20	25	30
RF (50)	84.1	85.7	91.5	82.1	88.6	76.1	0.78	0.79	0.87	0.74	0.83	0.67
RF (100)	84.6	85.1	91.1	82.1	88.2	76.1	0.78	0.79	0.87	0.72	0.83	0.67
RF (150)	84.1	85.1	91.1	82.6	88.2	73.9	0.78	0.79	0.82	0.74	0.82	0.63

IV. CONCLUSION

This study aims to classify land cover in the sugarcane area based on plant phenology knowledge. Classification is beneficial for the certainty of planting area and information on plant availability for the future. Classifying sugarcane areas was built using a Machine Learning approach and knowledge of plant phenology. In addition, in preprocessing segmentation with several segmentation scenarios. The classification results from the two comparisons that have been classified with phenological knowledge have better accuracy results. The accuracy obtained was 91.5%, and the kappa coefficient was 0.92 for size spacing ten and Random Forest trees 100 and 150. Suggestions for future research, optimization in conducting classification can be improved taking into account sharper satellite resolutions and Deep Learning algorithm approaches for more in-depth analysis.

ACKNOWLEDGMENT

We thank the Department of Informatics, Institut Teknologi Telkom Purwokerto, and the Department of Computer Science, IPB University, for supporting this research. We also thank the anonymous reviewers for their constructive comments and advice.

REFERENCES

[1] E. Respati, *Outlook Komoditas Perkebunan Tebu*. Indonesia: Pusat Data dan Sistem Informasi Pertanian Sekretaris Jenderal-Kementerian Pertanian, 2019.

[2] [BPS] Badan Pusat Statistik, *Indonesian Sugarcane Statistics 2018*, vol. 4, no. 1. 2019.

[3] A. C. Xavier, B. F. T. Rudorff, Y. E. Shimabukuro, L. M. S. Berka, and M. A. Moreira, "Multi-temporal analysis of MODIS data to classify sugarcane crop," *International Journal of Remote Sensing*, vol. 27, no. 4, pp. 755–768, 2006, doi: 10.1080/01431160500296735.

[4] C. Fortes and J. A. M. Demattê, "Discrimination of sugarcane varieties using Landsat 7 ETM+ spectral data," *International Journal of Remote Sensing*, vol. 27, no. 7, pp. 1395–1412, 2006, doi: 10.1080/01431160500383863.

[5] T. I. R. Almeida, C. R. De Souza Filho, and R. Rossetto, "ASTER and Landsat ETM+ images applied to sugarcane yield forecast," *International Journal of Remote Sensing*, vol. 27, no. 19, pp. 4057–4069, 2006, doi: 10.1080/01431160600857451.

[6] H. Lin, J. Chen, Z. Pei, S. Zhang, and X. Hu, "Monitoring sugarcane growth using ENVISAT ASAR data," *IEEE Transactions on Geoscience and Remote Sensing*, vol. 47, no. 8, pp. 2572–2580, 2009, doi: 10.1109/TGRS.2009.2015769.

[7] M. El Hajj, A. Bégué, S. Guillaume, and J. F. Martiné, "Integrating SPOT-5 time series, crop growth modeling and expert knowledge for monitoring agricultural practices - The case of sugarcane harvest on Reunion Island," *Remote Sensing of Environment*, vol. 113, no. 10, pp. 2052–2061, 2009, doi: 10.1016/j.rse.2009.04.009.

[8] B. F. T. Rudorff, D. A. de Aguiar, W. F. da Silva, L. M. Sugawara, M. Adami, and M. A. Moreira, "Studies on the rapid expansion of sugarcane for ethanol production in São Paulo state (Brazil) using Landsat data," *Remote Sensing*, vol. 2, no. 4, pp. 1057–1076, 2010, doi: 10.3390/rs2041057.

[9] J. R. Townshend, C. O. Justice, and V. Kalb, "Characterization and classification of South American Land cover types using satellite data," *International Journal of Remote Sensing*, vol. 8, no. 8, pp. 1189–1207, 1987, doi: 10.1080/01431168708954764.

[10] P. T. Wolter, D. J. Mladenoff, G. E. Host, and T. R. Crow, "Improved forest classification in the northern Lake States using multi-temporal Landsat imagery," *Photogrammetric Engineering and Remote Sensing*, vol. 61, no. 9, pp. 1129–1143, 1995.

[11] N. Gorelick, M. Hancher, M. Dixon, S. Ilyushchenko, D. Thau, and R. Moore, "Google Earth Engine: Planetary-scale geospatial analysis for everyone," *Remote Sensing of Environment*, vol. 202, no. 2016, pp. 18–27, 2017, doi: 10.1016/j.rse.2017.06.031.

[12] P. Griffiths, S. van der Linden, T. Kuemmerle, and P. Hostert, "A Pixel-Based Landsat Compositing Algorithm for Large Area Land Cover Mapping," *IEEE Journal of Selected Topics in Applied Earth Observations and Remote Sensing*, vol. 6, no. 5, pp. 2088–2101, 2013, doi: 10.1109/jstars.2012.2228167.

[13] T. Hermosilla, M. A. Wulder, J. C. White, N. C. Coops, and G. W. Hobart, "Disturbance-Informed Annual Land Cover Classification Maps of Canada's Forested Ecosystems for a 29-Year Landsat Time Series," *Canadian Journal of Remote Sensing*, vol. 44, no. 1, pp. 67–87, 2018, doi: 10.1080/07038992.2018.1437719.

[14] S. Sudianto and R. D. Wahyuningrum, "Identifikasi Sebaran Nitrogen pada Tanaman Padi Berbasis Pengetahuan Fenologi dan Remote Sensing," *Jurnal Nasional Pendidikan Teknik Informatika (Janapati)*, vol. 11, no. 3, pp. 166–175, 2022.

[15] A. Shalaby and R. Tateishi, "Remote sensing and GIS for mapping and monitoring land cover and land-use changes in the Northwestern coastal zone of Egypt," *Applied Geography*, vol. 27, no. 1, pp. 28–41, 2007, doi: 10.1016/j.apgeog.2006.09.004.

[16] M. A. Vieira, A. R. Formaggio, C. D. Rennó, C. Atzberger, D. A. Aguiar, and M. P. Mello, "Object Based Image Analysis and Data Mining applied to a remotely sensed Landsat time-series to map sugarcane over large areas," *Remote Sensing of Environment*, vol. 123, pp. 553–562, 2012, doi: 10.1016/j.rse.2012.04.011.

[17] Kumar Navulur, *Multispectral image analysis using the object-oriented paradigm*, vol. 53, no. 9. CRC Press/Taylor&Francis, 2006.

[18] M. P. dos Santos Silva, G. Camara, M. I. S. Escada, and R. C. Modesto de Souza, "Remote-sensing image mining: Detecting agents of land-use change in tropical forest areas," *International Journal of Remote Sensing*, vol. 29, no. 16, pp. 4803–4822, 2008, doi: 10.1080/01431160801950634.

[19] R. Achanta and S. Süsstrunk, "Superpixels and polygons using simple non-iterative clustering," *Proceedings - 30th IEEE Conference on Computer Vision and Pattern Recognition, CVPR 2017*, vol. 2017-Janua, no. Ic, pp. 4895–4904, 2017, doi: 10.1109/CVPR.2017.520.

[20] P. O. Gislason, J. A. Benediktsson, and J. R. Sveinsson, "Random forests for land cover classification," *Pattern Recognition Letters*, vol. 27, no. 4, pp. 294–300, 2006, doi: 10.1016/j.patrec.2005.08.011.

[21] Y. Jin, X. Liu, Y. Chen, and X. Liang, "Land-cover mapping using Random Forest classification and incorporating NDVI time-series and texture: a case study of central Shandong," *International Journal of Remote Sensing*, vol. 39, no. 23, pp. 8703–8723, 2018, doi: 10.1080/01431161.2018.1490976.

[22] [PTPN X] PT Perkebunan Nusantara X, "Optimizing Prime Commodities Management Through Synergy in Innovation," 2018.

[23] M. Boschetti, D. Stroppiana, P. A. Brivio, and S. Bocchi, "Multi-year monitoring of rice crop phenology through time series analysis of MODIS images," *International Journal of Remote Sensing*, vol. 30, no. 18, pp. 4643–4662, 2009, doi: 10.1080/01431160802632249.

[24] J. M. Pena-Barragan, M. K. Ngugi, R. E. Plant, and J. Six, "Object-based crop identification using multiple vegetation indices, textural features and crop phenology," *Remote Sensing of Environment*, vol. 115, no. 6, pp. 1301–1316, 2011, doi: 10.1016/j.rse.2011.01.009.

[25] S. Sudianto, Y. Herdiyeni, and L. B. Prasetyo, "Early Warning for Sugarcane Growth using Phenology-Based Remote Sensing by Region," *International Journal of Advanced Computer Science and Applications*, vol. 14, no. 2, 2023, doi: 10.14569/IJACSA.2023.0140259.

[26] D. S. Shumway, R.H., & Stoffer, *Time Series: A Data Analysis Approach Using R: A Data Analysis Approach Using R*. 2019.

[27] C. Padwick, M. Deskevich, F. Pacifici, and S. Smallwood, "WorldView-2 pan-sharpening," *American Society for Photogrammetry and Remote Sensing Annual Conference 2010: Opportunities for Emerging Geospatial Technologies*, vol. 2, pp. 740–753, 2010.

[28] R. S. Lunetta, J. F. Knight, J. Ediriwickrema, J. G. Lyon, and L. D. Worthy, "Land-cover change detection using multi-temporal MODIS NDVI data," *Remote Sensing of Environment*, vol. 105, no. 2, pp. 142–154, 2006, doi: 10.1016/j.rse.2006.06.018.

[29] R. P. Singh, N. Singh, S. Singh, and S. Mukherjee, "Normalized Difference Vegetation Index (NDVI) Based Classification to Assess the Change in Land Use/Land Cover (LULC) in Lower Assam, India," *International Journal of Advanced Remote Sensing and GIS*, vol. 5, no. 1, pp. 1963–1970, 2016, doi: 10.23953/cloud.ijarsg.74.

[30] M. C. Hansen, D. P. Roy, E. Lindquist, B. Adusei, C. O. Justice, and A. Altstatt, "A method for integrating MODIS and Landsat data for systematic monitoring of forest cover and change in the Congo Basin," Remote *Sensing of Environment*, vol. 112, no. 5, pp. 2495–2513, 2008, doi: 10.1016/j.rse.2007.11.012.

[31] J. R. B. Bwangoy, M. C. Hansen, D. P. Roy, G. De Grandi, and C. O. Justice, "Wetland mapping in the Congo Basin using optical and radar remotely sensed data and derived topographical indices," *Remote Sensing of Environment*, vol. 114, no. 1, pp. 73–86, 2010, doi: 10.1016/j.rse.2009.08.004.

[32] Sudianto, Y. Herdiyeni, and L. B. Prasetyo, "Machine learning for sugarcane mapping based on segmentation in cloud platform," presented at the The 3rd International Conference on Engineering, Technology and Innovative Researches, Purwokerto, Indonesia, 2023, p. 020001. doi: 10.1063/5.0132180.

[33] D. M. Chen and D. Stow, "The effect of training strategies on supervised classification at different spatial resolutions," *Photogrammetric Engineering and Remote Sensing*, vol. 68, no. 11, pp. 1155–1161, 2002.

[34] A. Tassi and M. Vizzari, "Object-Oriented LULC Classification in Google Earth Engine Combining SNIC, GLCM, and Machine Learning Algorithms," *Remote Sensing*, 2020, doi: doi.org/10.3390/rs12223776.

[35] M. Hall-Beyer, "Practical guidelines for choosing GLCM textures to use in landscape classification tasks over a range of moderate spatial scales," *International Journal of Remote Sensing*, vol. 38, no. 5, pp. 1312–1338, 2017, doi: 10.1080/01431161.2016.1278314.

[36] Z. Zhou *et al.*, "Object-oriented classification of sugarcane using time-series middle-resolution remote sensing data based on AdaBoost," *PLoS ONE*, vol. 10, no. 11, pp. 1–16, 2015, doi: 10.1371/journal.pone.0142069.

[37] T. Butkhot and P. Reungsang, "Asia - Pacific Journal of Science and Technology Assessment of machine learning on sugarcane classification using Landsat-8 and Sentinel-2 satellite imagery," pp. 1–11, 2021.